

General Disclaimer

One or more of the Following Statements may affect this Document

- This document has been reproduced from the best copy furnished by the organizational source. It is being released in the interest of making available as much information as possible.
- This document may contain data, which exceeds the sheet parameters. It was furnished in this condition by the organizational source and is the best copy available.
- This document may contain tone-on-tone or color graphs, charts and/or pictures, which have been reproduced in black and white.
- This document is paginated as submitted by the original source.
- Portions of this document are not fully legible due to the historical nature of some of the material. However, it is the best reproduction available from the original submission.

**NASA TECHNICAL
MEMORANDUM**

NASA TM X- 62,486

NASA TM X- 62,486

(NASA-TM-X-62486) MECHANICAL TEST IN-SITU
FRACTURE DEVICE FOR AUGER ELECTRON
SPECTROSCOPY (NASA) 17 p HC \$3.50 CSCL 11F

N76-11277

Unclas

G3/26 03080

**MECHANICAL TEST IN-SITU FRACTURE DEVICE FOR
AUGER ELECTRON SPECTROSCOPY**

R. Dale Moorhead

**Ames Research Center
Moffett Field, Calif. 94035**

September 1975



1. Report No. NASA TM X-62,486	2. Government Accession No.	3. Recipient's Catalog No.	
4. Title and Subtitle MECHANICAL TEST IN-SITU FRACTURE DEVICE FOR AUGER ELECTRON SPECTROSCOPY		5. Report Date	
		6. Performing Organization Code	
7. Author(s) R. Dale Moorhead		8. Performing Organization Report No. A-6273	
		10. Work Unit No. 506-16-11-02	
9. Performing Organization Name and Address NASA Ames Research Center Moffett Field, Calif. 94035		11. Contract or Grant No.	
		13. Type of Report and Period Covered Technical Memorandum	
12. Sponsoring Agency Name and Address National Aeronautical and Space Administration Washington, D. C. 20546		14. Sponsoring Agency Code	
		15. Supplementary Notes	
16. Abstract An in-situ fracture device for Auger spectroscopy is described. The device is designed to handle small tensile specimens or small double cantilever beam specimens and is fully instrumented with load and displacement transducers so that quantitative stress-strain measurements can be made directly. Some initial test results for specimens made from 4130 and 1020 steel are presented.			
17. Key Words (Suggested by Author(s)) In-situ fracture device Auger electron spectroscopy Fracture surface analysis		18. Distribution Statement UNLIMITED STAR Category - 26	
19. Security Classif. (of this report) UNCLASSIFIED	20. Security Classif. (of this page) UNCLASSIFIED	21. No. of Pages 16	22. Price* \$3.25

Mechanical test in-situ fracture device
for Auger electron spectroscopy

R. Dale Moorhead

Ames Research Center, NASA
Moffett Field, California 94035

Abstract

An in-situ fracture device for Auger spectroscopy is described. The device is designed to handle small tensile specimens or small double cantilever beam specimens and is fully instrumented with load and displacement transducers so that quantitative stress-strain measurements can be made directly. Some initial test results for specimens made from 4130 and 1020 steel are presented.

INTRODUCTION

The analysis of fracture surface chemistry has been one of the more fruitful applications of Auger electron spectroscopy (AES). Since the importance of doing the fracture in-situ to avoid contamination has been emphasized repeatedly, this success, at least in part, has been due to the availability and utilization of in-situ fracture devices. Probably the most popular in-situ fracture apparatus for AES is a commercial model that is designed to fracture small, notched bar specimens by impact loading. The reported cases where this device was used are many, attesting to the fact that it has been and will continue to be a most useful tool. However, impact loading to failure is a high-rate fracture process while many real material failures are controlled by time-dependent mechanisms such as creep-rupture, fatigue, stress-corrosion, and hydrogen embrittlement. Thus, there

is a wide range of time-dependent problems that can utilize the impact fracture techniques in only a secondary way. Additionally, when one is attempting to correlate some important change in mechanical strength with fracture surface chemistry by AES, it would be much more desirable (and more economical) if one could determine the fracture properties of the specimen directly in-situ.

For these reasons, it was decided to design and construct a new fracture apparatus that would permit the in-situ fracture and AES examination of a variety of specimen types under well-controlled, measurable test conditions. The following is a description of the device which consists of a main load frame and a pair of multiple specimen holders; one holder is designed for use with small tensile specimens, and the other for small double-cantilever beam (DCB) specimens.

DESCRIPTION OF APPARATUS

The point of departure for the design of the fracture mechanism was an existing screw-bellows assembly mounted on a 6-in. (15.24-cm) OD ultra-high vacuum flange. The former use of this assembly is not known, but it is doubtful that even with prior purpose one could have designed a more suitable vacuum assembly for a fracture apparatus. Ruggedly constructed, with a heavy duty 5/8-8 Acme screw, the mating nut works against a ball thrust bearing enclosed in a housing that keeps the system in alignment.

In addition to developing a scheme for moving the specimens into and out of the mechanism, the principal consideration in converting the apparatus into a fracture device was to design a load frame that would complement the high stiffness and load capacity of the existing assembly.

This finally took the shape of a cylinder which is seen detached and sitting upright in Fig. 1(a). The cylinder is machined from high-grade steel and is bored to a size just large enough to permit it to slip over the bellows sleeve of the vacuum assembly and come to rest against the inside surface of the vacuum flange, as shown in Fig. 1(b). Slots and openings machined into the closed end of the cylinder at various locations and directions are for loading and alignment of the specimen. The specimen is gripped by dowel pins pressed into holes in the specimen ends. Figure 2 is a cutaway view of the apparatus as it appears with a tensile specimen in the loaded position. The free end of the specimen is fed into the apparatus through the horizontal and vertical slots in the bottom half of the load-frame cylinder and springs up to be caught by the yoke attached to the bellows and screw. For DCB specimens, the yoke shown attached in Figs. 1(a) and 2 is replaced by a clevis type with a fixed pin shown unattached in Fig. 1(a). The DCB specimen is manipulated into the assembly in such a way that the "hook" side of the specimen is caught by the clevis pin. A DCB is shown in the loaded position in Fig. 1(b).

In order to measure load, a compression washer was installed and is held in position between the thrust bearing and body of the assembly by a centering bushing. The washer is thus compressed by the load on the screw. A rotary potentiometer that engages a gear attached to the nut serves as a displacement transducer. A convenience item added to the system is a constant-torque, variable-speed motor. The motor is coupled to the fracture assembly by pulley and cord as seen in Fig. 1(c). Thus, load-displacement curves like that shown in Fig. 3 for a 1020 tensile specimen can be recorded as a matter of routine.

The multiple specimen carousels, one for each kind of specimen, are shown in Figs. 4(a) and 4(b). Each carousel holds four specimens that are attached to the carousel by small bolts. The carousels attach to the sting of the standard motion feedthrough supplied with the Auger equipment (PHI Model 10-502). As shown in the figures, each carousel has one fractured specimen shown in the attitude assumed for Auger analysis. In this attitude the fracture surfaces can be positioned at the focus of the CMA (and optical microscope) for analysis. There is enough travel in the motion feedthrough to analyze the entire length of the fracture surface of DCB specimens. The final component added to the Auger spectrometer, needed to make the overall system operational, was a "wobble stick" motion feedthrough of commercial design that is used to flip individual specimens around as required for loading into the fracture unit. In Fig. 1(c), this is the device with the black knob mounted on the small access port located between the large window port and the fracture apparatus.

PRELIMINARY APPLICATION AND DISCUSSION

The first systematic use to be made of this new capability will be the study of the fracture characteristics and fracture surface chemistry of mild steel tensile specimens that have been subjected to various degrees of hydrogen attack, that is, attack that occurs with exposure to high-temperature, high-pressure hydrogen. Such information, along with the qualitative analysis of gases that may evolve during plastic deformation or fracture of the specimen (as measured by quadrupole residual gas analysis) may lead to a greater insight into the mechanism of hydrogen attack. However, during the development of the apparatus, and mostly for the purposes of testing its operation, specimens of both DCB and tensile configurations have been fractured and analyzed. For example, DCB specimens of AISI 4130 steel, heat treated to a yield strength of 1330 MNm^{-2} , were fractured in a vacuum of $4 \times 10^{-7} \text{ Pa}$ ($3 \times 10^{-9} \text{ torr}$) and in

a 665 Pa (50 torr) atmosphere of hydrogen according to the following routine. After the specimens were heat treated, a fatigue crack was initiated in air, using a conventional tensile testing machine, and advanced about 2 mm. The specimens were then sand blasted, degreased, mounted on the specimen carousel, and installed in the Auger system. After bakeout, out-gassing, etc., the specimens were manipulated into the fracture device and fractured. In the case of vacuum fracture, the load necessary to advance the crack was achieved by using the motorized drive to increase the displacement slowly. In the case of the hydrogen atmosphere, the specimens were preloaded to a point somewhat below that needed to advance the crack and then the system was back-filled with hydrogen to the stated pressure. The embrittling effect of the hydrogen was sufficient to cause the crack to propagate to complete failure without further displacement of the screw.

As might be expected, exposing a fresh fracture surface to an atmosphere of 665 Pa (50 torr) of hydrogen causes substantial changes in its surface chemistry as determined by AES. This is demonstrated for a 4130 specimen in Figs. 5(a) and 5(b). Figure 5(a) shows the spectrum, taken as soon after fracture as possible, from the surface of a specimen fractured in a vacuum of 4×10^{-7} Pa (3×10^{-9} torr). This spectrum is to be compared to the one in Fig. 5(b) taken from the same area after being exposed to a hydrogen environment similar to that used to cause embrittlement. This simple exposure to hydrogen has caused substantial changes. The iron peak at 47 eV has been greatly reduced and appears to have split into two peaks; the sulphur peak is diminished (but still ample) as is the carbon and there has been a large increase in the oxygen signal. The spectrum in Fig. 5(c) was taken from the same area as those shown in 5(a) and 5(b) after etching the sample for 3 min with argon ions; it demonstrates that the effects of the hydrogen environment can be effectively removed by just a small amount of ion bombardment.

It seems evident, therefore, that insofar as contamination is concerned the fracture surface chemistry of specimens actually fractured in such a hydrogen atmosphere would also be affected in the same manner. However, the foregoing results would encourage one to think that ion etching would again produce a surface that is nearly chemically equivalent to an uncontaminated surface. A spectrum from such a surface is shown in Fig. 5(d). This spectrum was taken from a specimen that was fractured (by embrittlement) in hydrogen, then ion etched for 3 min. Except for the absence of sulphur, it is almost identical to that shown in Figs. 5(a) and 5(c). (Except for sulphur, a spectrum very similar to that in Fig. 5(b) was recorded just prior to ion etching.) Thus, from a chemical point of view, sulphur seems to distinguish a vacuum-fractured surface from a hydrogen-fractured surface. This observation has been verified on repeated occasions during the course of this work. Scanning electron fractography of the surfaces shows the characteristic dimpled morphology of ductile failure for those specimens fractured in vacuum (Fig. 6(a)) and the delineated grain structure morphology of intergranular fracture for those tested in hydrogen (Fig. 6(b)).

This correlation of sulphur with a ductile mode of fracture is in accord with the findings of Cox and Low.¹ Working with 4340 steel, they concluded that plastic fracture occurred by the nucleation and growth of voids formed by the fracture of the interface between sulfide inclusions and the matrix. Accordingly, the fracture path more or less follows the dispersion of these inclusions within the fracture zone and consequently sulphur bearing particles become a prominent feature of the fracture surface. In terms of surface chemistry, this has the effect of concentrating sulphur at the fracture surface in amounts that are surely in excess of the stereological equivalent amounts of a randomly dispersed bulk distribution that the heat treatment of the specimen

was supposed to produce. In the case of the hydrogen-fractured specimen, this mechanism of concentration is absent because the fracture path is defined by the grain boundaries and, although an occasional sulfide may be encountered here, the amount of sulphur present on such surfaces is frequently below that detectable by Auger spectroscopy. Marcus and Harris have recently expressed a similar opinion regarding sulfide inclusions and the part they play in ductile fracture.²

Another interesting observation concerns the Auger analysis of the 1020 tensile specimen used to obtain the load displacement curve shown in Fig. 3. This specimen was machined from a commercial grade of 1020 steel and was tested in vacuum without further heat treatment. Thus, the exact thermal history of the specimen is not known. Partial Auger scans from the fracture surface of this specimen are shown in Fig. 7. The first scan (Fig. 7(a)) was taken at 4×10^{-7} Pa (3×10^{-9} torr) as soon after fracture as possible. The focus of the following discussion will be on the phosphorous that shows up in this spectrum. Like sulphur, phosphorous is a common impurity in steels like 1020 but is usually present in even lower concentrations than sulphur. Thus, finding phosphorous in the spectrum must also imply some mechanism for its concentration at the surface. Unlike sulphur (which is frequently enhanced by ion etching), ion etching for less than 3 min causes a complete disappearance of the phosphorous signal (Fig. 7(b)). Except for chemical species, this very same phenomenon has been reported by Marcus and Harris.² They reported the presence of arsenic on the fracture surface of a 1018 steel specimen in a zone that had failed in the ductile mode. They were able to cause the complete disappearance of the arsenic Auger signal by removing as little as 20 Å of the surface by ion etching. They explained this by observing that in their specimen the arsenic occupied a very narrow zone at the carbide matrix interface causing a weakness for the fracture

path to follow. Thus, upon fracture this narrow zone in the bulk becomes a thin layer covering the carbide particles and is rapidly etched away by ion bombardment. Perhaps this same explanation holds for the phosphorous in the present case. In any event, the carbon signal (with a shape indicating a carbide chemistry) is substantially enhanced by a little ion etching, a fact that (Fig. 7(b)) would be in accord with such an explanation.

CONCLUSIONS

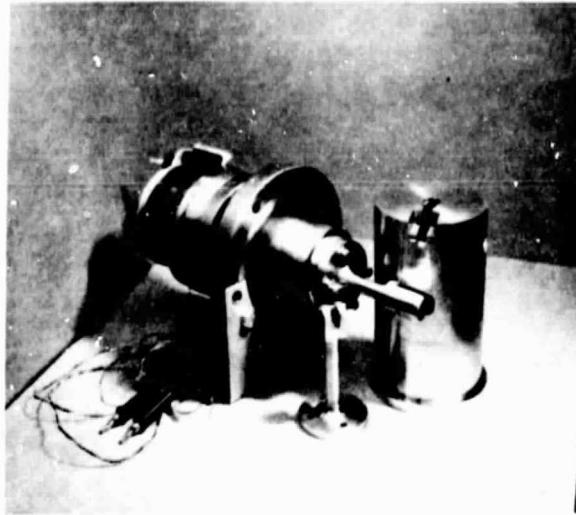
The results presented above demonstrate the workability of the fracture apparatus described herein. They also demonstrate the broad utility of the apparatus by showing how it can be used to produce, in-situ, a variety of fracture surfaces including those produced by environmentally induced slow-crack growth. We think it is significant that we can interpret our Auger results along lines already suggested because they bear upon the mechanisms of plastic fracture whereas in the past, most Auger studies have been concerned with intergranular failure and grain boundary phenomena.

ACKNOWLEDGEMENTS

The author wishes to acknowledge the priority of Professor R. P. Wei and Dr. G. W. Simmons of Lehigh University for the design and construction of apparatus similar in concept to that described herein and to thank them for providing us with descriptive material of their equipment.

¹T. B. Cox and J. R. Low, Jr., *Met. Trans.* 5, 1457 (1974).

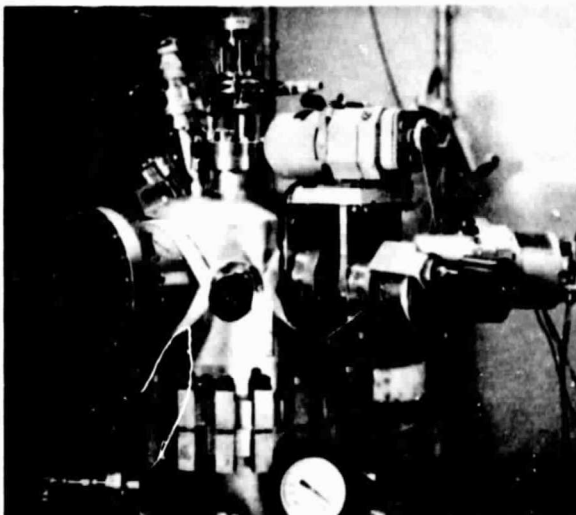
²H. L. Marcus and J. M. Harris, *Scripta Met.* 9, 563 (1975).



(a)



(b)



(c)

Figure 1.— (a) Fracture device partially disassembled. The large cylinder is the load frame. The extra (unattached) clevis with the pin is used for the DCB type of specimen. (b) Fully assembled with a DCB specimen in the loaded position. (c) General view of Auger spectrometer with fracture attachment installed.

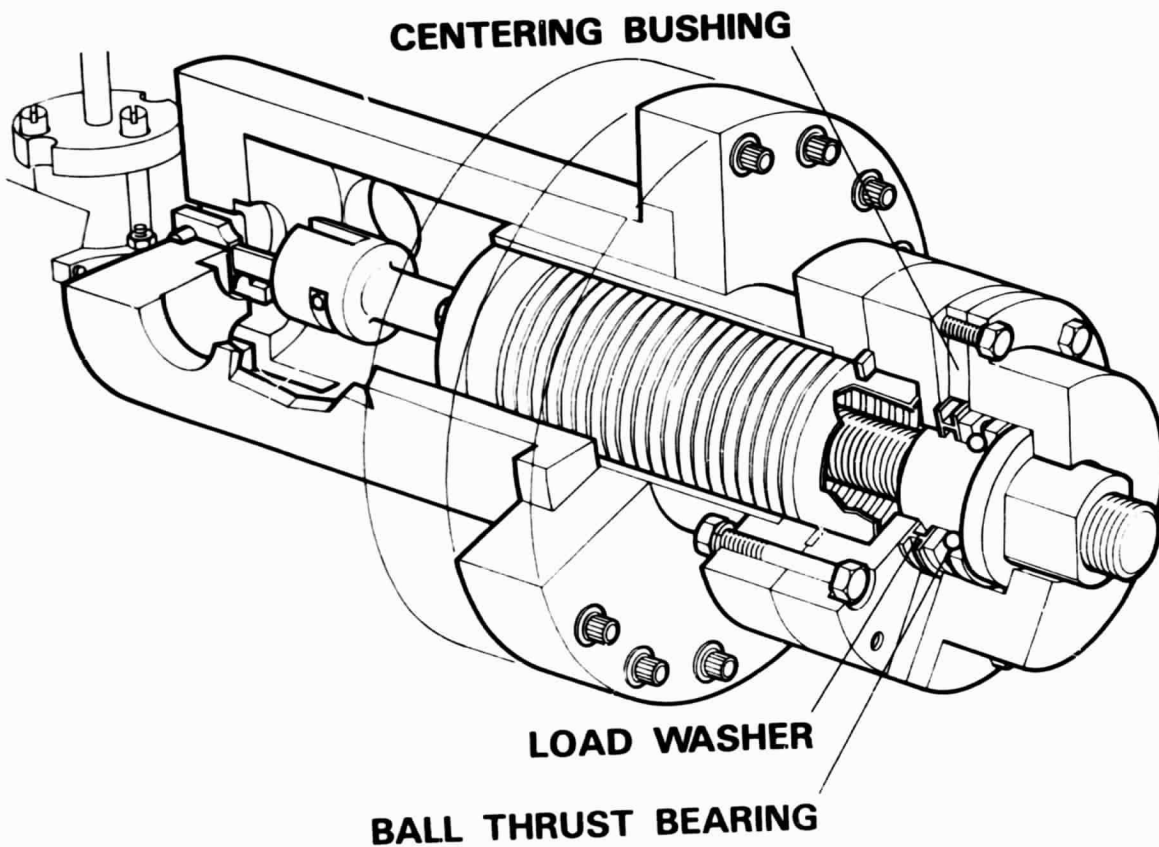


Figure 2.— Artist's drawing of a mechanical test fracture device for Auger electron spectroscopy.

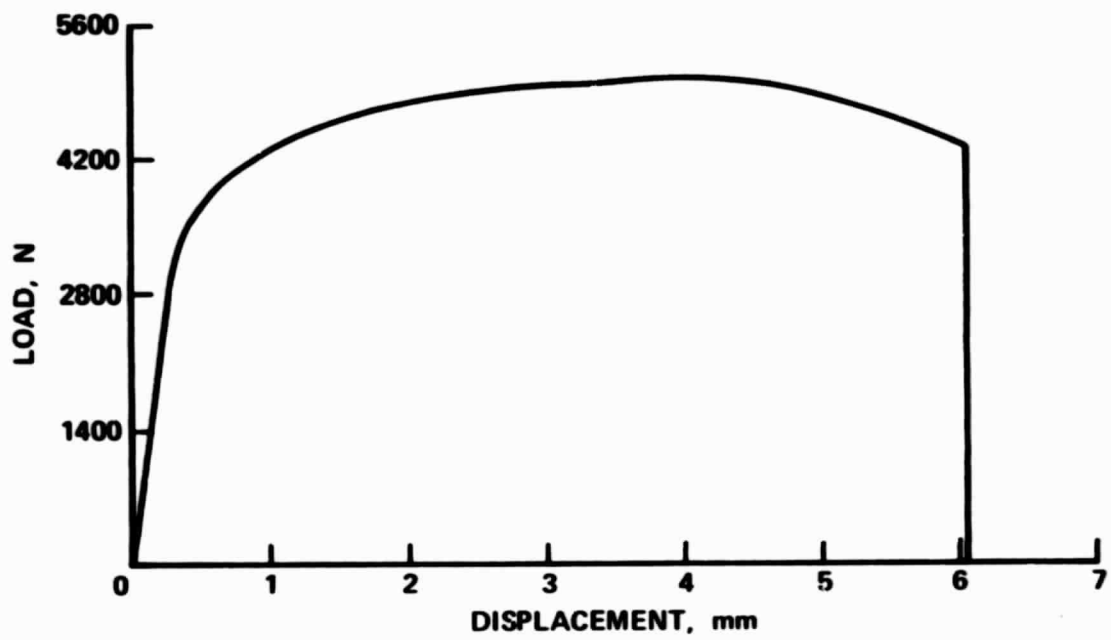
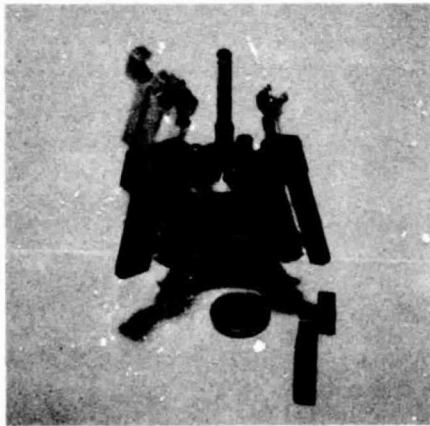
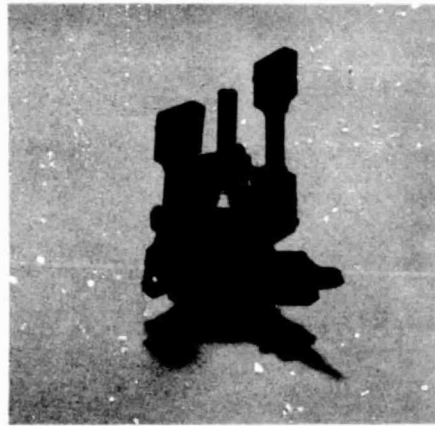


Figure 3.— Load-displacement curve for a 1020 tensile specimen.



(a)



(b)

Figure 4.— Specimen carousels: (a) for DCB type showing two halves of one that has been fractured; (b) for tensile specimen, with one fractured.

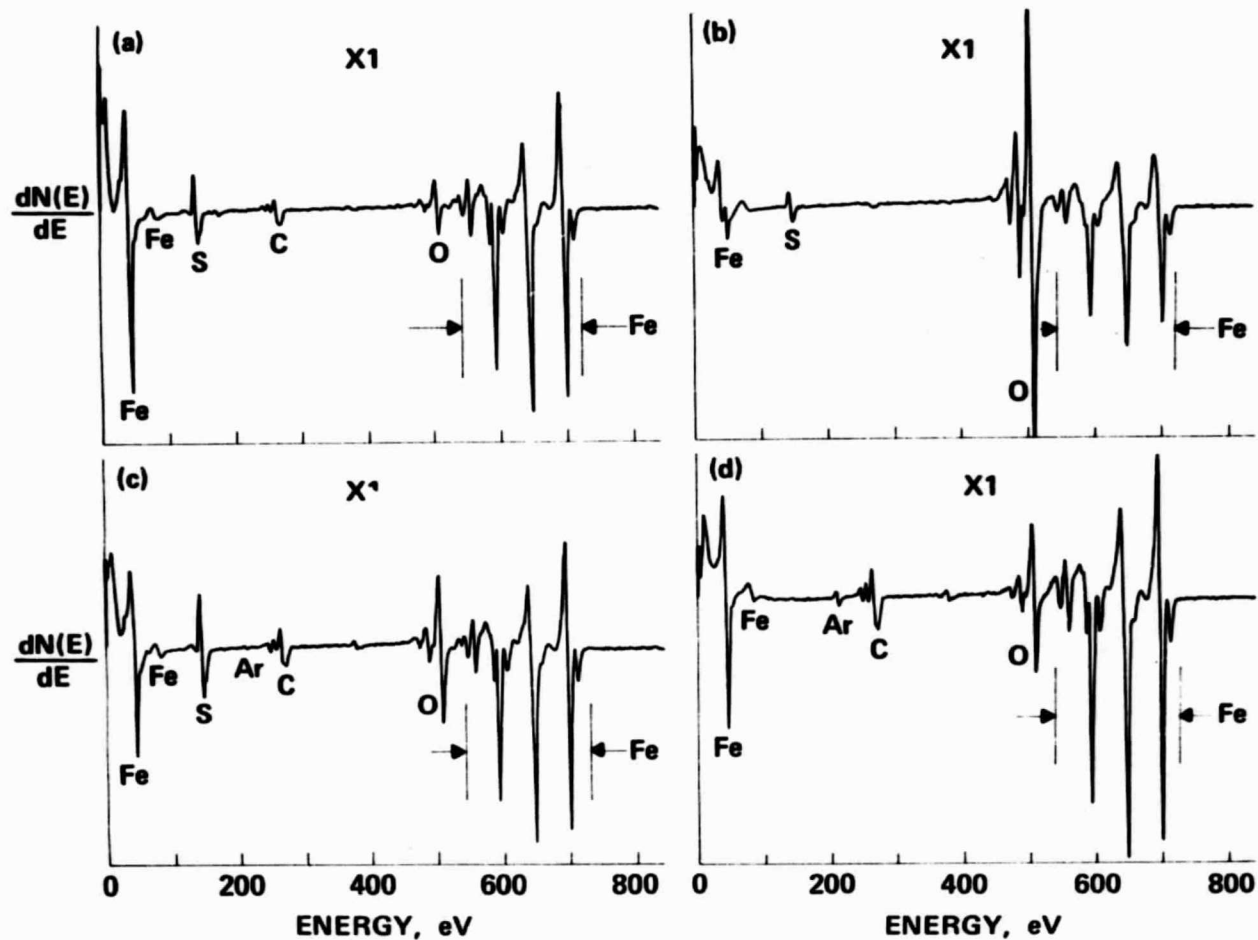


Figure 5.— Auger spectra taken from fracture surface of a 4130 DCB specimen. (a) Fractured in vacuum, taken as soon after fracture as possible. (b) Same as (a) after being exposed to a 665 Pa (50 torr) hydrogen atmosphere. (c) Same as (a) and (b) after being ion etched for 3 min. with argon ions. (d) From a 4130 specimen fractured in hydrogen after ion etching for 3 min.

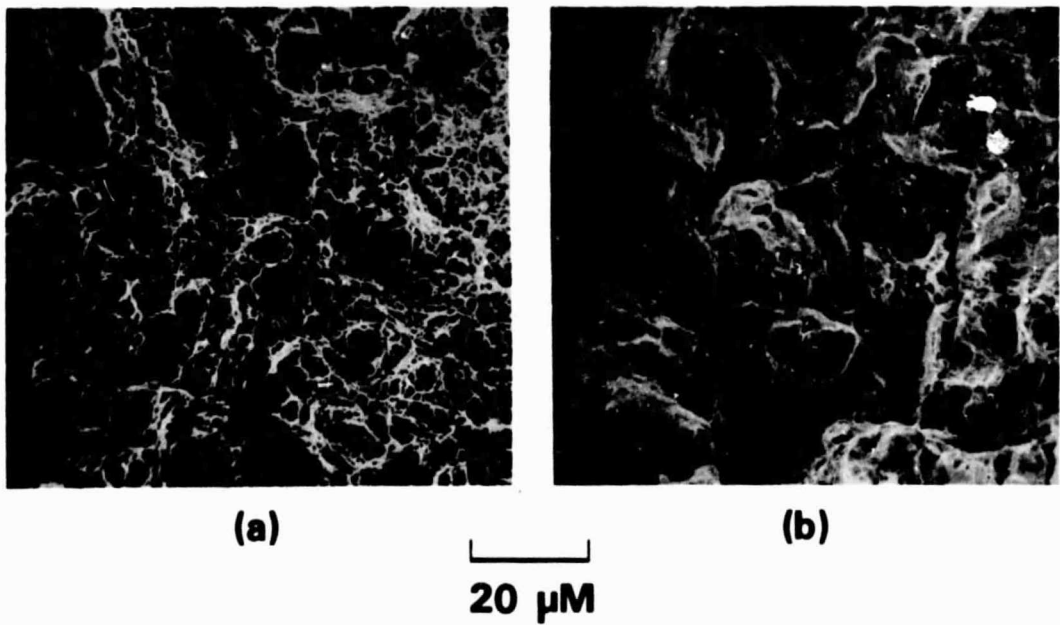


Figure 6.— Electron micrographs of a 4130 DCB fracture surface, (a) fractured in vacuum, (b) fractured in hydrogen.

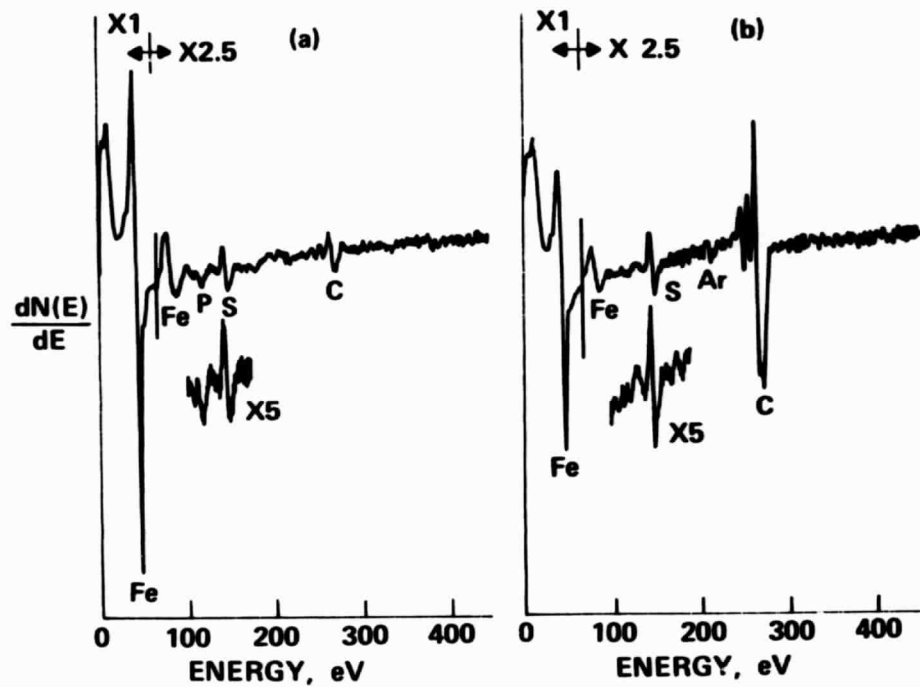


Fig. 7

Figure 7.— Auger spectra taken from a 1020 tensile specimen fractured in vacuum: (a) as soon after fracture as possible; (b) same as (a) after ion etching for 3 min.